Disease progression promotes changes in adipose tissue signatures in type 2 diabetic (*db/db*) mice: The potential pathophysiological role of batokines

Khanyisani Ziqubu[1], Phiwayinkosi V. Dludla[2,3], Marakiya T. Moetlediwa[1,2], Thembeka A. Nyawo[2,4], Carmen Pheiffer[2,4,5], Babalwa U. Jack[2], Bongani B. Nkambule[6], Sithandiwe E. Mazibuko-Mbeje[1]

[1]Department of Biochemistry, North-West University, Mmabatho 2745, South Africa.

[2]Biomedical Research and Innovation Platform, South African Medical Research Council, Tygerberg 7505, South Africa.

[3]Department of Biochemistry and Microbiology, Faculty of Science and Agriculture, University of Zululand, KwaDlangezwa 3886, South Africa.

[4]Centre for Cardio-Metabolic Research in Africa, Division of Medical Physiology, University of Stellenbosch, Tygerberg 7505, South Africa.

[5]Department of Obstetrics and Gynaecology, Faculty of Health Science, University of Pretoria, Pretoria 0001, South Africa.

[6]School of Laboratory Medicine and Medical Sciences, University of KwaZulu-Natal, Durban 4000, South Africa.

Corresponding author:

Sithandiwe E. Mazibuko-Mbeje, PhD

Department of Biochemistry, Faculty of Natural and Agricultural Sciences, North West University, Mafikeng Campus, Private Bag X 2046, Mmabatho 2735, South Africa.

E-mail address: 36588296@nwu.ac.za

Abstract

Unlike the white adipose tissue (WAT) which mainly stores excess energy as fat, brown adipose tissue (BAT) has become physiologically important and therapeutically relevant for its prominent role in regulating energy metabolism. The current study makes use of an established animal model of type 2 diabetes (T2D; *db/db* mice) to determine disease progression affects adipose tissue morphology and gene regulatory signatures within this animal model of T2D. Results showed that WAT and BAT from *db/db* mice display a hypertrophied phenotype that is consistent with increased expression of the pro-inflammatory cytokine, tumor necrosis factor-alpha *(Tnf-α)*. Moreover, BAT from both *db/db* and non-diabetic control mice displayed an age-related impairment in glucose homeostasis, inflammatory profile, and thermogenic regulation, as demonstrated by reduced expression of genes like glucose transporter (GLUT)-4, adiponectin *(AdipoQ),* and uncoupling protein 1 *(Ucp-1)*. Importantly, gene expression of the batokines regulating sympathetic neurite outgrowth and vascularization, including bone morphogenic protein 8b *(Bmp8b),* fibroblast growth factor 21 (*Fgf-21)*, neuregulin 4 *(Nrg-4)* were altered in BAT from *db/db* mice. Likewise, gene expression of meteorin-like *(Metrnl)*, growth differentiation factor 15 *(Gdt-15)*, and C-X-C motif chemokine-14 *(Cxcl-14)* regulating pro- and anti-inflammation were impaired. This data provides some new insights into the pathophysiological mechanisms involved in BAT hypertrophy (or whitening) and the disturbances of batokines during the development and progression of T2D. However, these are only preliminary results as additional experiments are necessary to confirm these findings in other experimental models of T2D.

Keywords: Brown adipose tissue; Batokines; Obesity; Type 2 diabetes

1. Introduction

Type 2 diabetes (T2D) remains one of the leading causes of death, with the International Diabetes Federation estimating that was responsible for more than 6.7 million global deaths in the year 2021 [1]. The classical features of T2D include hyperglycemia and insulin resistance, with the latter acknowledged as being mostly facilitated by the rapid rise in the cases of obesity [1]. Diverse risk factors such as aging, smoking, and a sedentary lifestyle are considered essential etiological factors implicated in the development of T2D [2,3]. However, obesity, which is consistent with excessive ectopic fat accumulation and insulin resistance is currently considered to be the major risk for developing T2D [4]. The size and quality of adipose tissue depots may be the critical determinants of the overall health of people with obesity [5,6]. This consequence becomes worse with the progression of the disease, as the adipose tissue eventually becomes dysfunctional, favoring an increased production of pro-inflammatory factors [7]. There is a close association between excessive fat accumulation and increased infiltration of macrophages which can drive systemic metabolic dysfunction, hyperglycemia, and other related metabolic complications [8,9].

The rapid rise in cases of obesity and related metabolic complications has highlighted a need to clarify the pathological role of adipose tissue during the development of T2D [10–12]. Humans are known to present with three types of adipose tissue with distinct morphology and function, which become important to study. Firstly, the white adipose tissue (WAT) contains fewer mitochondria but a large unilocular lipid droplet, which is necessary for the storage of excess energy in a form of fat. Secondly, the brown adipose tissue (BAT) has more mitochondria and is considered a thermoregulatory tissue for promoting energy expenditure [13]. Beige adipose tissue (bAT) is the third and relatively new type of adipose tissue that is derived from WAT but under thermogenic stimulations resemble BAT [14]. Interestingly, exploration of BAT/bAT in adult humans has reignited interest in targeting these tissues for their importance in energy regulation and glucose homeostasis [15–17]. Effective interventions against T2D like physical activity can target the conversion of WAT to BAT, in a process that promotes energy expenditure by making use of stored fat [18]. Indeed, BAT has the unique capacity to convert excess or reserved energy, which is stored as fat, into heat by promoting mitochondrial oxidative phosphorylation and the process called thermogenesis [19].

Therefore, it has become evident that BAT and bAT play an endocrine function, by secreting batokines that exert a fundamental influence on metabolic regulation [20]. These distinct characteristics remain essential for alleviating pathological features of obesity and metabolic syndrome [21–24]. Thus, the present study aimed to

provide the morphological characterization of inguinal WAT and interscapular BAT remodeling, as well as changes in BAT/bAT-derived factors during the development and progression of obesity and T2D in *db/db* mice.

2. Materials and Methods

The Ethical Committee of the South African Medical Research Council (SAMRC) approved the study protocol (ECRA 13/19), which followed the principles and guidelines of the SAMRC on Ethics for Medical Research: Animal use in research and training https://www.samrc.ac.za/research/ethics/guideline-documents.

2.1. Animal care and study design

Male C57BL/KsJ-Lepr homozygous leptin receptor-deficient diabetic (*db/db*) mice and their heterozygous leptin-receptor-deficient non-diabetic (*db/+*) littermate controls (Jackson's Laboratories, Bar Harbor, USA) were housed at the Primate Unit and Delft Animal Centre (PUDAC) of the SAMRC. The mice were kept in a controlled environment with a temperature of 23-25ºC, relative humidity of ~50%, and a 12-hour light/dark cycle, and received standard laboratory chow pellets (Afresh Vention, Cape Town, South Africa) *ad libitum* and had free access to drinking water. Mice (total of n=60) were assigned to six different experimental groups (n = 10/each group) based on age, as follows: 8-,12-, and 18-weesk-old *db/+* and *db/db* mice (**Fig. 1**).

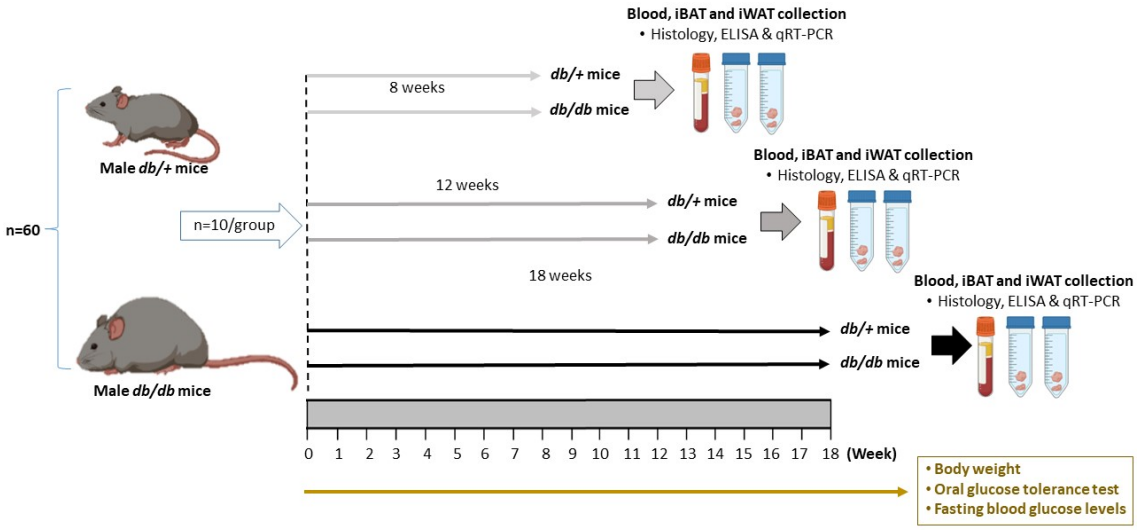

Figure 1: An overview of the experimental design. A total of 60 male *db/db* mice and their control littermates *db/+* mice were monitored from the age of 8-, 12-, and 18-weeks. Body weights, Oral Glucose Tolerance Test, and fasting blood glucose levels were determined or performed weekly. Subsequently, insulin resistance was

calculated using the Homeostasis Model of Assessment for Insulin Resistance. At pre-determined experiment time points, animals were sacrificed to collect blood, inguinal WAT (iWAT) and the interscapular BAT (iWAT). These tissues were used for histological analysis, as well as gene expression analysis using enzyme-linked immunosorbent assay (ELISA) and quantitative real time PCR (qRT-PCR).

2.2. Measurement of body weights and oral glucose tolerance test

The body weights and fasting glucose concentrations were measured on a weekly basis. At the pre-determined experiment time (i.e. 8-, 12-, and 18 weeks) points, oral glucose tolerance test (OGTT) was performed, in which after a 12-h fast, 1 g/kg dextrose solution was administered by animals via oral gavage. Subsequently, fasting blood glucose levels were measured using a Contour plus glucometer (Ascensia, Basel, Switzerland) through tail pricking at time intervals of 0, 30, 60, and 120 min.

2.3. Animal sacrifice and collection of samples

The sacrifice of animals at weeks 8, 12, and 18, involved a 12-h fast before being anaesthetized using isoflurane (Sigma-Aldrich, St. Louis, MO, USA) and terminated by exsanguination from the vena cava. Blood was collected into serum separator tubes from Becton, Dickinson, and Company (Franklin Lakes, New Jersey, United States), allowed to clot, and then centrifuged at 4000 g for 20 min. Subsequently, serum was aliquoted and stored frozen at -80°C for further analysis. Inguinal WAT and interscapular BAT were excised, cleaned with 10 × Dulbecco's phosphate buffered saline (Lonza; Maryland, United States); and weighed. A portion of the tissues was fixed in 10% formalin for histological analysis, and the other remaining parts were immersed in RNA later from Invitrogen (Carlsbad, California, United States) and later stored at -25ºC for gene expression quantification.

2.4. Histological analysis

Sections of fixed iWAT and iBAT were cut at 4 μm thickness using a Leica RM2125 rotary microtome (Leica Microsystems; Nussloch, Germany) and mounted on Histobond® microscope glass slides (Marienfeld, Lauda-Königshofen, Germany). Thereafter, the mounted tissues were placed in an oven at 60 °C for 1-h and stained with haematoxylin and eosin (H&E). Digital images were captured using an OLYMPUS BX50 microscope (Olympus Corporation; Tokyo, Japan) at a 20 X magnification for at least five random fields per slide. Thereafter, the adipocyte area was measured using the Image-J software with the Adiposoft plugin.

2.5. Biochemical analysis

Biochemical markers such as insulin and glucose transporter (GLUT)-4 levels were measured in the serum and iBAT using commercially available enzyme-linked immunosorbent assay (ELISA) kits as per the manufacturer's instructions. Accordingly, fasting insulin levels were measured using the mouse insulin enzyme-linked immunosorbent assay (ELISA) kit, as per the manufacturer's instructions (Merck; Darmstadt, Germany). Thereafter, the Homeostasis Model of Assessment for Insulin Resistance (HOMA-IR), as a determinant of insulin resistance, was calculated according to the formula: fasting insulin (μU/L) x fasting glucose (nmol/L) / 22.5 [25]. Furthermore, the quantity of glucose transporter (GLUT)-4 in iBAT was measured using R&D Systems mouse DuoSet® ELISA kit (Minneapolis, Minnesota, United States), according to the manufacturer's instructions.

2.6. Real-time quantitative polymerase chain reaction (RT-PCR)

To extract the total ribonucleic acid (RNA), about 30-100 mg of fat tissue kept in RNA later was transferred to a 1 mL TRIzol™ lysis reagent from Invitrogen (Carlsbad, California, United States) and homogenized at 25 Hz for 1 min (x4 repeats). Subsequently, a Nanodrop™ One spectrophotometer from Thermo Fisher Scientific (Waltham, Massachusetts, United States) was used to determine the concentration and purity of RNA. Complementary DNA (cDNA) was synthesized from RNA 150 ng RNA using the High-Capacity cDNA Reverse Transcription kit from Applied Biosystems (Foster City, California, United States), according to the manufacturer's instructions. TaqMan gene expression assays (**Table 1**) and TaqMan Universal PCR Master Mix (Thermo Fisher Scientific, Waltham, United States) were used to amplify cDNA by quantitative real-time PCR (qRT-PCR) on a QuantStudio™ 7 Flex Real-Time PCR system (Applied Biosystems) under the following conditions: 95°C for 20 sec, followed by 40 cycles of 95°C for 1 sec and 60°C for 20 sec. Transcription levels were quantified using the comparative CT, delta-delta (ΔΔCT), and the actin beta *(Act-β)* gene was used as an endogenous control to normalize the expression of the target genes. Due to the unavailability of the tissues or fewere tissues for 12 weeks-old mice, the gene expression analysis of the tumor necrosis factor-alpha *(Tnf-α)* was only assessed in 8 weeks-old mice (young; early phase of T2D) and 18 weeks-old mice (aged; late phase of T2D).

Table 1. TaqMan™ gene expression assays.

Gene	Gene symbol	Assay ID
Adiponectin	*AdipoQ*	Mm00456425-m1
Bone morphogenetic protein 8b	*Bmp8b*	Mm 00432115_g1
Actin beta	*Act-β*	Mm02619580_g1
C-X-C motif chemokine ligand 14	*Cxcl-14*	Mm 00444699_m1
Fibroblast growth factor 21	*Fgf-21*	Mm 00840165_g1
Growth differentiation factor 15	*Gdf-15*	Mm 00442228_m1
Meteorin like protein	*Metrnl*	Mm 00522681_m1
Neuregulin 4	*Nrg-4*	Mm 00446254_m1
Tumor necrosis factor-alpha	*Tnf-α*	Mm00443258_m1
Vascular endothelial growth factor A	*Vegf-A*	Mm 01281449_m1
Uncoupling protein 1	*Ucp-1*	Mm01244861_m1

2.7. Statistical analysis

The two-way analysis of variance (ANOVA) was used followed by Tukey's post hoc multiple tests in GraphPad Prism software, version 8.0.2 (San Diego, California, United States). Unpaired Student's t-test or Mann-Whitney test was used for two-group comparisons. The results were presented as the means ± standard error of the mean (SEM), n = 10 mice per group. The p-value of < 0.05 was considered statistically significant.

3. Results

3.1. Age-related changes in body weight, glucose tolerance, and insulin sensitivity levels in *db/db* mice

The measured general physiological parameters included body weights, fasting blood glucose, and fasting insulin levels, as well as determination of insulin resistance using HOMA-IR, for the period of 8-, 12-, and 18 weeks (**Table 2**). As expected, *db/db* mice displayed significantly increased body weights than *db/+* controls, in an age-dependent manner, $p < 0.0001$ (**Fig. 1A**). Moreover, this was consistent with raised blood glucose levels, also displaying an age-dependent increase $p < 0.0001$ (**Fig. 1B**). Also, *db/db* mice showed significantly increased insulin levels than *db/+* controls, however, the levels of insulin were significantly reduced in *db/db* mice with age, $p < 0.0001$ (**Fig. 1C**). To indicate a characteristic feature of T2D, the *db/db* mice displayed significantly increased insulin resistance, $p < 0.0001$ (**Fig. 1D**) and glucose intolerance, $p < 0.0001$ (**Fig. 1E**) as determined by increased HOMA-IR and OGTT respectively.

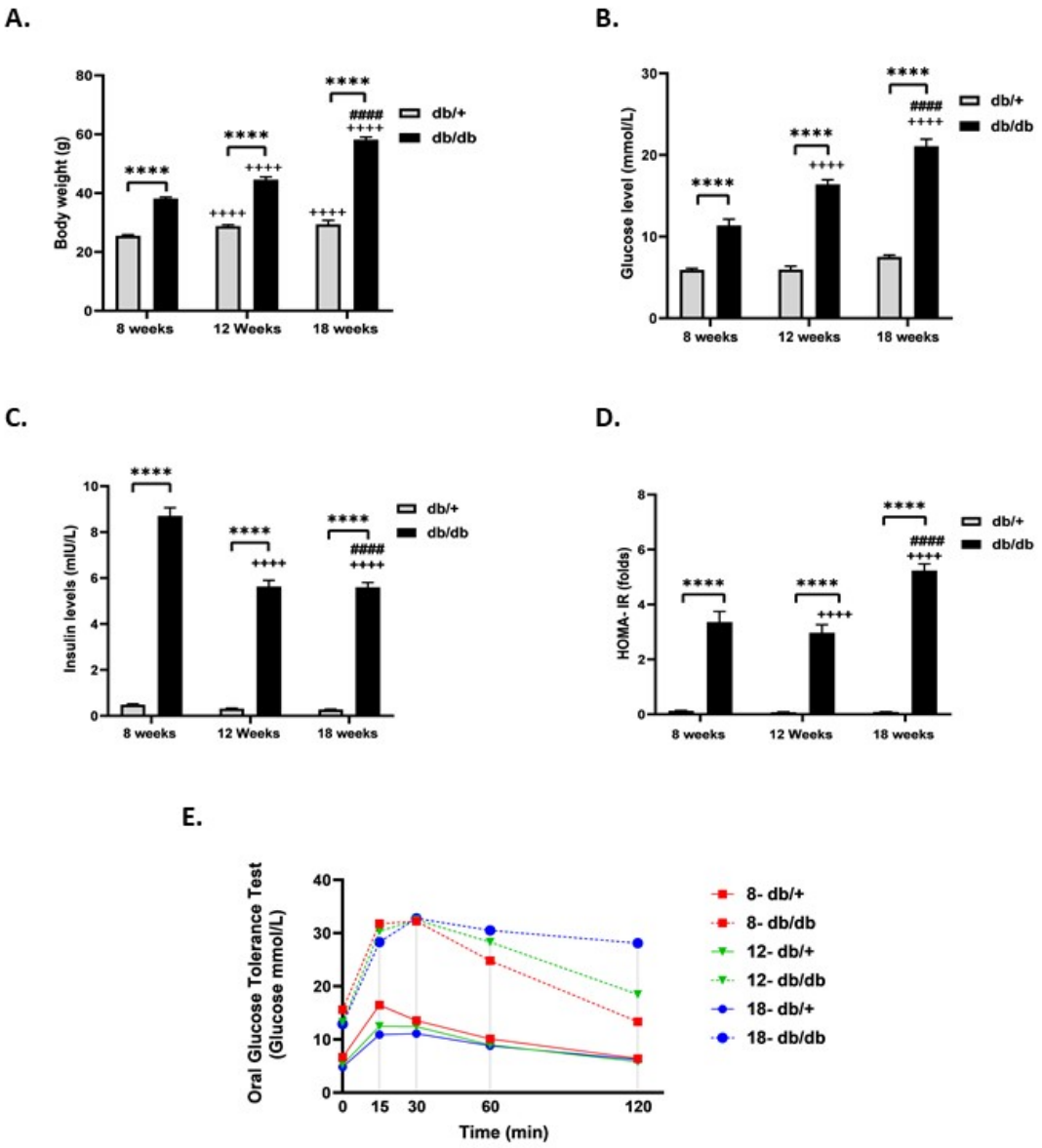

Figure 2: Changes in (A.) Body weight, (B.) Fasting blood glucose, (C.) Fasting insulin levels, (D.) Insulin sensitivity as measured by the Homeostasis Model of Assessment for Insulin Resistance (HOMA-IR), and (E.) Oral Glucose Tolerance Test (OGTT) in 8-, 12-, and 18-week-old *db/db* mice. Results are expressed as the mean ± SEM (n=10). Significant differences are indicated as follows: **** $p < 0.0001$ vs all *db/+* controls; $^{++++}$ $p < 0.0001$ 12-week-old mice and 18-week-old mice (*db/+* and *db/db*) vs 8-week-old *db/+* controls; and $^{\#\#\#\#}$ $p < 0.0001$ 18-week-old mice (*db/+* and *db/db*) vs 12-week-old *db/+* controls.

3.2. Age-related hypertrophy and pro-inflammatory cytokine expression in inguinal WAT from the *db/db* mice

The histological results demonstrated that the iWAT was hypertrophied in *db/db* mice from 8 to 18 weeks (**Fig. 2A**). Originally, iWAT depot as shown in the lean group has both multilocular "brown/beige adipocytes" and unilocular "white adipocyes" lipid droplets, iWAT accumulated more unilocular lipid droplets in *db/db* mice (**Fig 2A**). To confirm this, the adipocytes area was measured, and it showed a significant increase in iWAT adipocytes size of *db/db* mice from 8 to 18 weeks, ($p < 0.0001$) (**Fig. 2B**). With clear increases in fat mass accumulation in iWAT from *db/db* mice, we next measured the expression levels of the most well studied pro-inflammatory cytokine, tumor necrosis factor-alpha *(Tnf-α)* in iWAT at early (8 weeks) and late phase (18 weeks) of the disease progression. Expression of the *(Tnf-α)* gene, was significantly increased in iWAT from *db/db* mice at 8- and 18-weeks with $p = 0.0244$ and $p < 0.0010$, respectively (**Fig. 2C**). By 18 weeks, lean control *db/+* mice also displayed slight elevations in the expression of this cytokine although it was not significant (**Fig. 2C**).

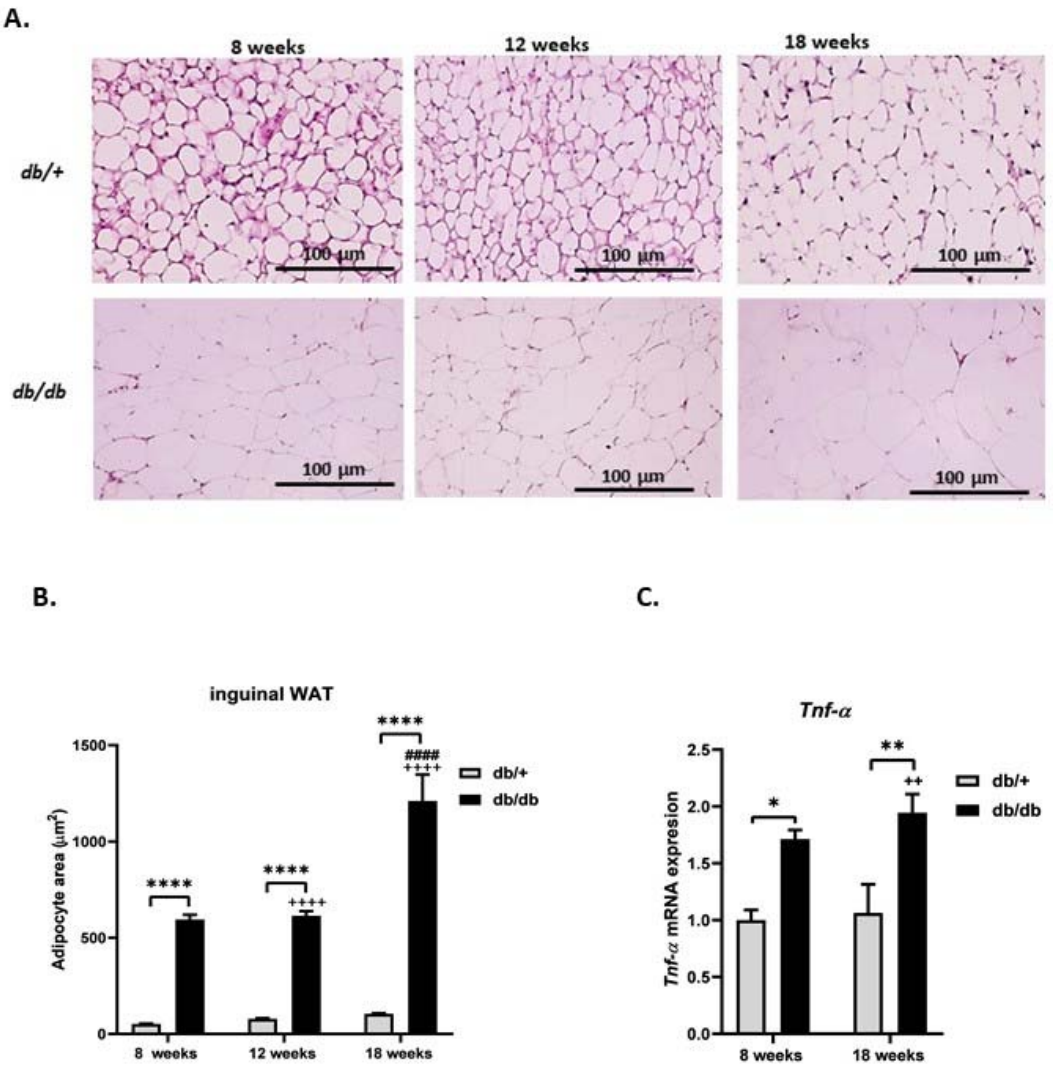

Figure 3: Morphological changes and pro-inflammatory response in the inguinal white adipose tissue (iWAT) from 8-, 12-, and 18-weeks old *db/+* and *db/db* mice. (A.) Representative histological images of iWAT at 10× magnification, (B) graphical representation of iWAT adipocytes area, and (C.) tumor necrosis factor-alpha (*Tnf-α*) expression as a classical pro-inflammatory marker. Results are represented as mean ± SEM (n=10). * $p < 0.05$, ** $p < 0.01$, **** $p < 0.0001$ vs all *db/+* controls; $^{++}$ $p < 0.01$, $^{++++}$ $p < 0.0001$ 12-week-old mice and 18-week-old mice (*db/+* and *db/db*) vs 8-week-old *db/+* controls; and $^{####}$ $p < 0.0001$ 18-week-old mice (db + and *db/db*) vs 12-week-old *db/+* controls.

3.3. Age-related BAT hypertrophy (or whitening) and pro-inflammatory cytokine expression in *db/db* mice

The histological examination was also performed to visualize the morphological changes in the iBAT from 8-,12-, and 18-weeks old *db/db* mice (**Fig. 4A**). Here, iBAT from *db/db* reprogramed phenotypically from smaller multilocular brown adipocytes to larger unilocular white-like adipocytes (**Fig. 4A**). This was corroborated by a significant increase in adipocytes area, $p < 0.0001$ (**Fig. 4B**), as a determinant of adipocyte hypertrophy. The latter was linked with the significant increase in *Tnf-α* expression in BAT from 18-weeks old *db/db* mice, $p = 0.0089$ (**Fig. 4C**).

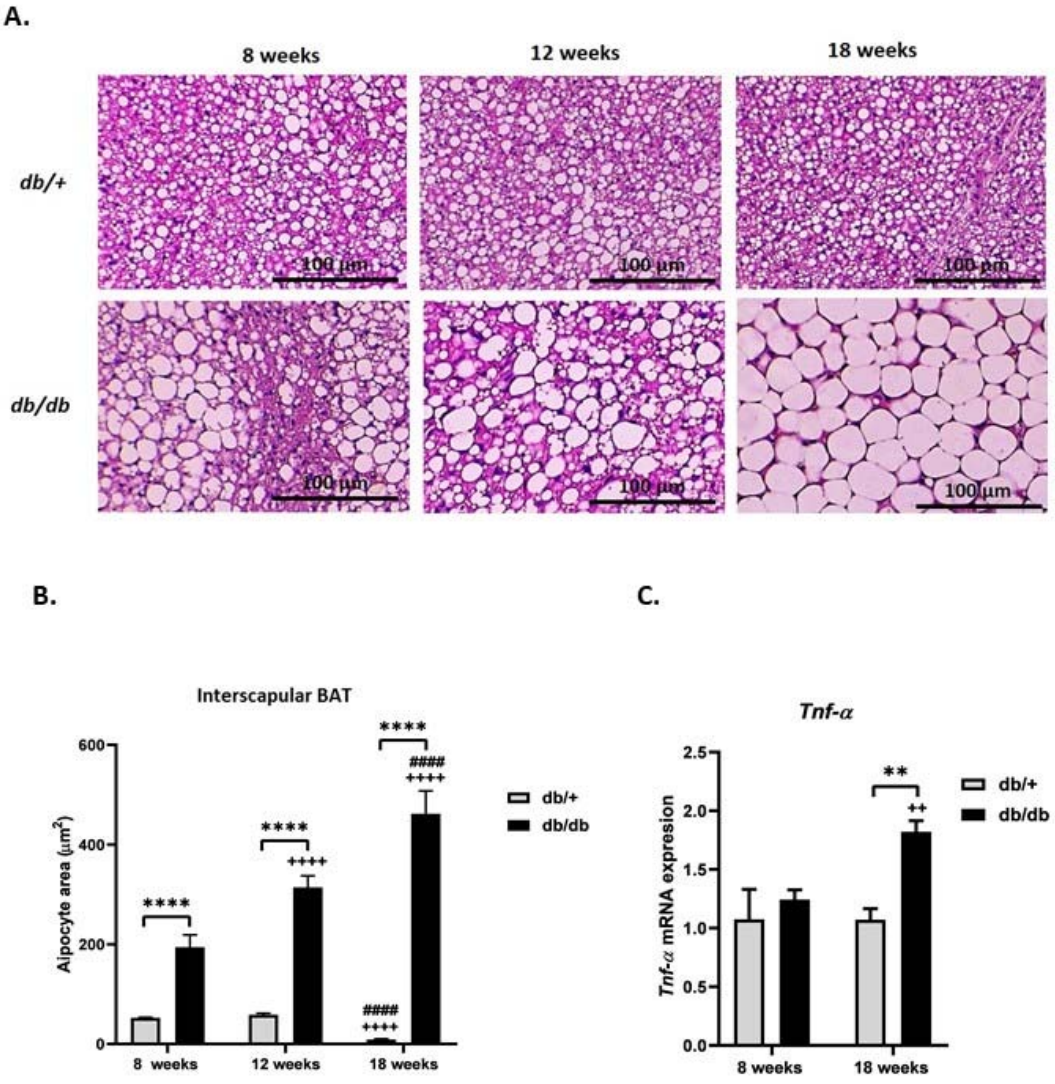

Figure 4: Morphological changes and pro-inflammatory response in the interscapular brown adipose tissue (iBAT) from 8-, 12-, and 18-weeks old *db/+* and *db/db* mice. (A.) Representative histological images of iBAT at 10× magnification, (B) graphical representation of iBAT adipocytes area, and (C.) tumor necrosis factor-alpha (*Tnf-α*) expression as a pro-inflammatory marker. Results are represented as mean ± SEM (n=10). ** $p < 0.01$, **** $p < 0.0001$ vs *db/+* controls; $^{++}$ $p < 0.01$, $^{++++}$ $p < 0.0001$ 12-week-old mice and 18-week-old mice (*db/+* and *db/db*) vs 8-week-old *db/+* controls; and $^{\#\#\#\#}$ $p < 0.0001$ 18-week-old mice (*db* + and *db/db*) vs 12-week-old *db/+* controls.

3.4. Age-related impairment in genes regulating glucose metabolism and thermogenic machinery in BAT from *db/db* mice

To elucidate the gene regulatory mechanisms underlying the impaired thermogenic function of iBAT in *db/db* mice during the different weekly stages of growth, expression levels of glucose transporter 4 (GLUT-4), adiponectin (*AdipoQ*), and uncoupling protein 1 (*Ucp-1)* were measured (**Fig. 5**). The results showed that GLUT-4 was significantly reduced in iBAT from 8-, 12-, and 18-weeks- old ($p < 0.0001$) *db/db* mice compared to *db/+* mice (**Fig. 5A**). This was correlated with the significant decrease in the expression of *AdipoQ*, an adipokine that promotes glucose metabolism, at 12-weeks ($p < 0.0001$) and 18-weeks ($p < 0.0001$) in *db/db* mice (**Fig. 5B**). Moreover, there was a significant decrease in *Ucp-1* expression at 8-weeks ($p < 0.0001$), 12-weeks ($p < 0.001$), and 18 weeks ($p < 0.01$) in *db/db* mice (**Fig. 5C**).

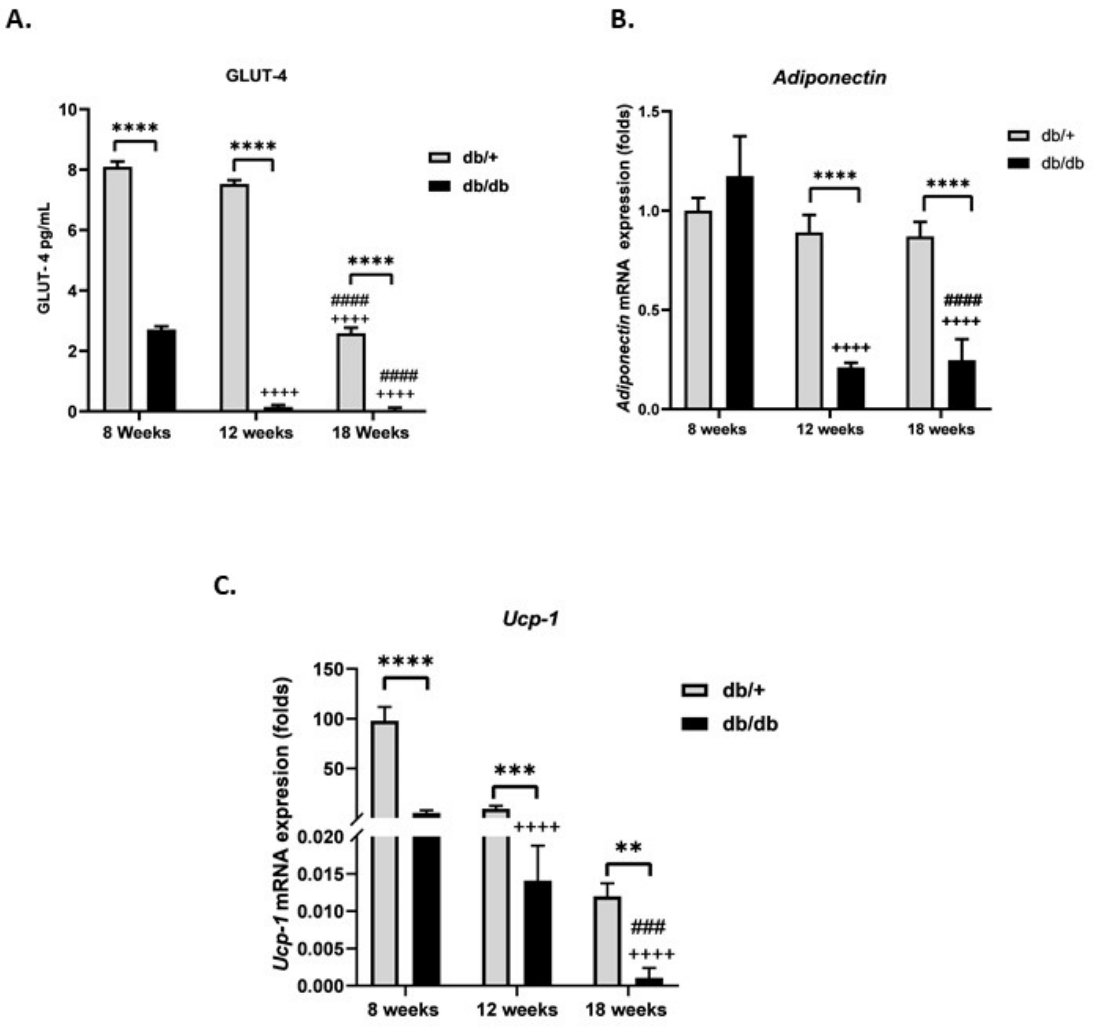

Figure 5: Impaired gene expression of (A.) glucose transporter (GLUT)-4, (B.) adiponectin (*AdipoQ*), (C.) uncoupling protein 1 *(Ucp-1)* in the interscapular brown adipose tissue (iBAT) from 8-, 12-, and 18-weeks *db/+* and *db/db* mice. Results are expressed as the mean ± SEM (n=10). Significant differences are indicated as follows: ****$p < 0.0001$ vs all *db/+* controls, and $^{++++}$ $p < 0.0001$ 12-week-old mice and 18-week-old mice (*db/+* and *db/db*) vs 8-week-old *db/+* controls, and $^{\#\#\#\#}$ $p < 0.0001$ 18-week-old mice (*db/+* and *db/db*) vs 12-week-old *db/+* controls.

3.5. Age-related impairment in gene expression of neuro-vasculature regulating batokines *Bmp8b, Fgf-21, Nrg-4,* and *Vegf-A* in iBAT from *db/db* mice

Consistent with the defect in thermogenesis, the expression pattern of BAT secreted signaling molecules "batokines" encoding genes involved in sympathetic nerve activation and vascularization from the iBAT of 8-, 12-, and 18-weeks old obese diabetic *db/db* mice were analyzed (**Fig. 6**). Accordingly, bone morphogenetic

protein 8b *(Bmp8b)* expression was significantly decreased in 8-weeks ($p < 0.0001$), 12-weeks ($p < 0.0001$) and 18 weeks ($p = 0.0430$) *db/db* mice (**Fig. 6A**). Likewise, the expression of fibroblast growth factor 21 *(Fgf-21)* was significantly decreased in all *db/db* groups; 8-weeks ($p < 0.002$), 12-weeks ($p < 0.0067$), and 18-weeks ($p < 0.0001$) (**Fig. 6B**). Interestingly, neuregulin 4 *(Nrg-4)* expression was significantly decreased in iBAT from *db/db* mice at 8-weeks ($p < 0.0103$), then followed by significant decrease at 12-weeks ($p = 0.0106$) and 18 weeks ($p = 0.0224$) *db/db* mice (**Fig. 6C**). Furthermore, vascular endothelial growth factor A *(Vegf-A)* was significantly decreased in iBAT from *db/db* mice at 12- ($p = 0.0381$) and 18- ($p = 0.0459$) weeks-old while there was no significant change at 8 weeks implying that vascularization was not affected at the early phase of the disease progression (**Fig. 6D**).

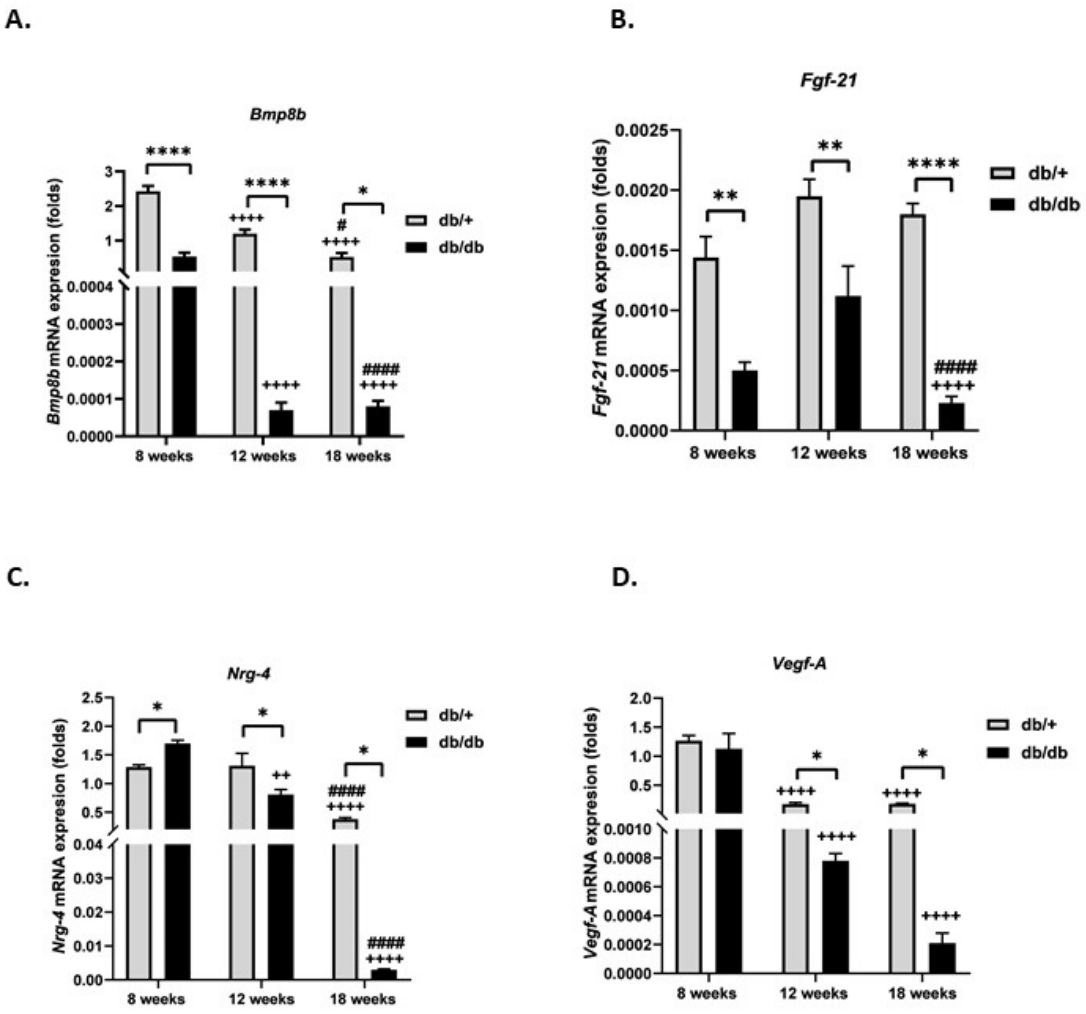

Figure 6: Impaired gene expression of (A.) bone morphogenic protein 8b *(Bmp8b),* (B.) fibroblast growth factor 21 (*Fgf-21)*, (C.) neuregulin 4 *(Nreg-4),* and (D.) vascular endothelial growth factor-A (*Vegf-A)* in the interscapular brown adipose tissue (iBAT) from 8-, 12-, and 18-weeks-old *db/+* and *db/db* mice. Results are

expressed as the mean ± SEM (n=10). Significant differences are indicated as follows: *p < 0.05, **p < 0.01, **p < 0.001, ****p < 0.0001 vs *db/+* controls, and $^{++}$ p < 0.01 $^{++++}$ p < 0.0001 12-week-old mice and 18-week-old mice (*db/+* and *db/db*) vs 8-week-old *db/+* controls; and $^{\#}$p < 0.05, $^{\#\#\#\#}$ p < 0.0001 18-week-old mice (*db* + and *db/db*) vs 12-week-old *db/+* controls.

3.6. Age-related impairment in gene expression of inflammation regulating batokines *Cxcl-14, Gdf-15,* and *Metrnl* in iBAT from *db/db* mice

While there was no significant change in the expression of C-X-C motif chemokine ligand 14 *(Cxcl-14)* in iBAT from *db/db* mice at 8 weeks, a significant decrease at 12 weeks (p =0.0066) and 18 weeks (p <0.001) was observed (**Fig. 7A**). Likewise, growth differentiation factor 15 *(Gdf-15)* expression was significantly increased in 12 weeks- (p =0.0146) and 18 weeks (p <0.001) old *db/db* mice while there was no prominent change at 8 weeks (**Fig. 7B**). Furthermore, expression of meteorin like *(Metrnl)* in both *db/+* and *db/db* showed a significant decreased with age-increase (**Fig. 7C**). Notably, *db/db* mice showed a significant decrease in *Metrnl* expression at 8-weeks (p =0.0069), 12-weeks (p =0.0048) and 18 weeks (p =0.0026) relative to *db/+* mice (**Fig. 7C**).

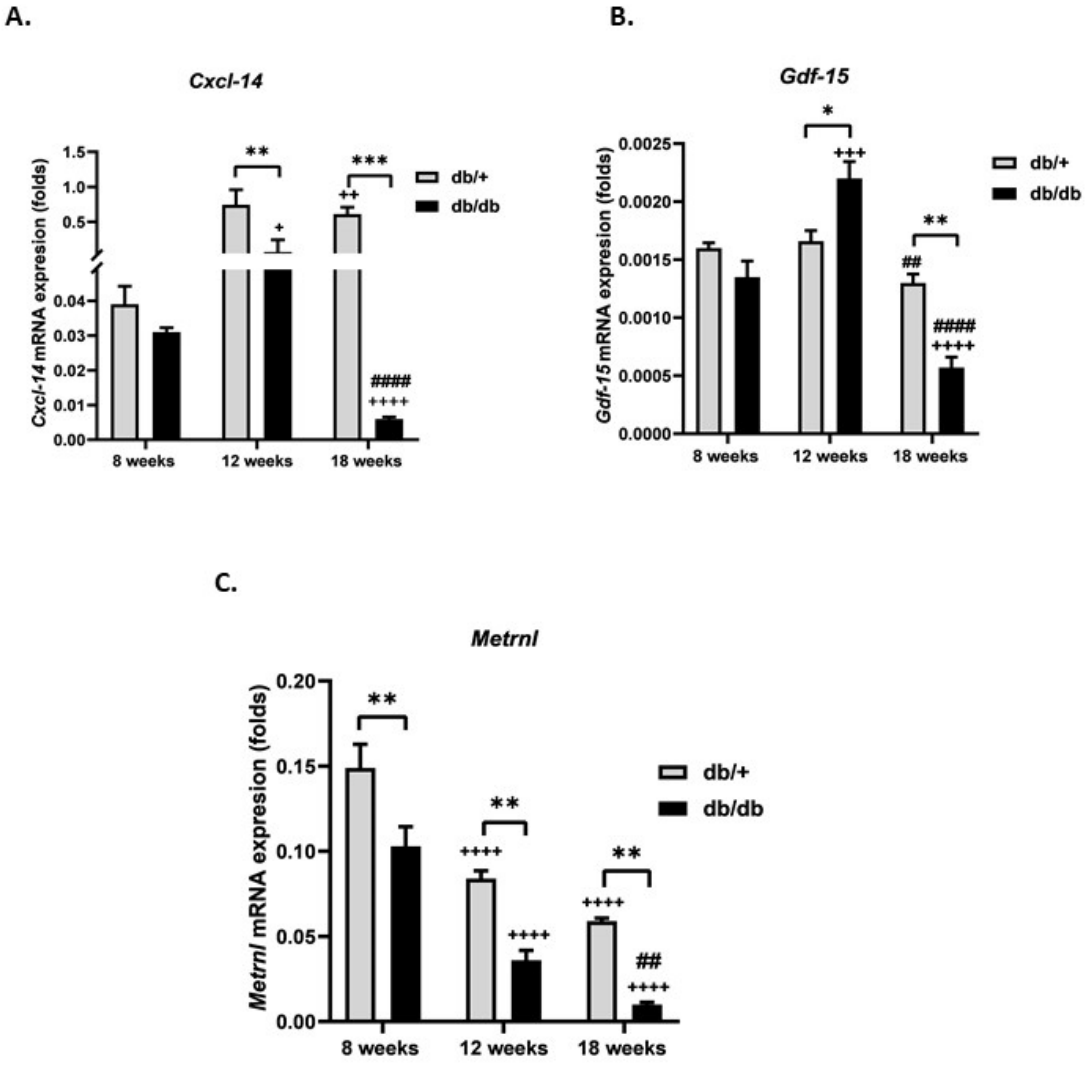

Figure 7: Impaired gene expression of (A.) meteorin-like (*Metrnl),* (B.) growth differentiation factor 15 (*Gdt-15),* and (C.) C-X-C motif chemokine-14 *(Cxcl-14)* in the interscapular brown adipose tissue (iBAT) from 8-, 12-, and 18-weeks old *db/+* and *db/db* mice. Results are expressed as the mean ± SEM (n=10). Significant differences are indicated as follows: *p < 0.05, **p < 0.001, ***p < 0.001, ****p < 0.0001 vs *db/+* controls, and $^{+}$p < 0.05, $^{++}$ p < 0.001 $^{++++}$ p < 0.0001 12-week-old mice and 18-week-old mice (*db/+* and *db/db*) vs 8-week-old *db/+* controls, and $^{\#\#}$p < 0.001, $^{\#\#\#\#}$ p < 0.0001 18-week-old mice (*db/+* and *db/db*) vs 12-week-old *db/+* controls.

4. Discussion

BAT can undergo a profound conversion to "white-like" phenotype with age, a classical feature defined as "age-related BAT whitening" [26,27]. Most worryingly, the progressive BAT whitening occurs concurrently with

disturbances in glucose metabolism in a preclinical model of a high-fat diet [28]. Such changes are also consistent with altered batokines gene expression, reduced nonshivering thermogenesis, and body temperature, leading to low energy expenditure. This has become imperative to understand since the secretion of batokines by the BAT is instrumental in the regulation of energy metabolism and efficient metabolic function [20,29]. Although the loss of BAT through whitening is quite common during obesity and progression of T2D [30,31], little is known about batokines, as potential molecular markers of obesity and T2D. Hence, observing changes in BAT-derived factors is very important for a better understanding of the underlying pathogenesis of various metabolic diseases.

The results herein have demonstrated that worsening of the diabetic state promotes adiposity and BAT hypertrophy, with the increased pro-inflammatory cytokine *Tnf-α* and concomitant loss of *Ucp-1* expression in *db/db* mice, an animal model of obesity and T2D that displays an age-dependent progression of T2D with early insulin resistance followed by insulin secretory defects [32,33]. Likewise, inguinal WAT displayed hypertrophy which was accompanied by increased *Tnf-α* expression. This is in line with the previous research demonstrating that worsened diabetic state is consistent with adipose tissue dysfunction and chronic inflammation marked by increased pro-inflammatory cytokines and decreased anti-inflammatory genes in mice and humans [34,35]. In addition, increased inflammation, and oxidative stress in BAT from obese mice have been previously reported [36]. It is well accepted that BAT is a potential therapeutic target for obesity and T2D which can be attributable to its capacity to oxidize fatty acids and glucose for thermogenesis sustainability [37,38]. The current experimental model already displayed predominant characteristic features of T2D, since all animals presented with an age-dependent increase in body weight, impaired glucose clearance, and insulin resistance, as previously reported [39,40]. Moreover, the expression of the genes regulating glucose metabolisms like GLUT-4 and *AdipoQ* were suppressed in BAT from *db/db* mice with worse results seen at 18-weeks of age. Which implies that worsening of the diabetic condition within *db/db* mice (as previously described [41]) may lead to the development of several metabolic dysregulations including impaired glucose metabolism. Nevertheless, previous research has already indicated that the expression levels of prominent genes involved in glucose and lipid metabolism like GLUT-4 and adiponectin are significantly affected by disease progression[42–46]. In fact, reduced expression levels are even worse in adipocytes when compared to other tissues like the skeletal muscle, which could explain significantly lower mRNA expression levels for GLUT4, adiponectin, UCP1 within BAT of *db/db* mice when compared to the controls [42–46].

Several lines of evidence suggest that BAT whitening is driven by multiple factors, including impairment of the sympathetic nervous system, vascular rarefraction, and altered endocrine signals, each of which is capable of

inducing macrophage infiltration and brown adipocyte death [47–49]. In agreement with the latter, our data has demonstrated an impairment of *Bmp8b, Nrg-4,* and *Vegf-A* expression in BAT in *db/db* mice, implying that the age-related progression of T2D is linked with the impaired sympathetic nervous system (neurite outgrowth), vascularization, and thermogenesis. It has been reported that BAT-secreted *Bmp8b* promotes sympathetic innervation via *Nrg-4* and its deletion results in impaired metabolic rate and increased weight gain in C57Bl6/J mice [50,51], whereas *Nrg-4* protects against diet-induced insulin resistance and hepatic steatosis by attenuating hepatic lipogenesis in mice [52]. Another study has reported that targeted deletion of *Vegf-A* in adipose tissue of non-obese mice results in BAT whitening, which supports a decreased vascularity in BAT of an obese subject [53]. Our data also showed that expression of *Fgf-21* was progressively reduced in iBAT of *db/db* mice. This is in line with the recent findings from Serdan et al. [54] showing that the expression of *Fgf-21* was decreased in insulin-resistant obese Wistar and T2D Goto-Kakizaki rats, with evidence of a whitening process in these animals. In terms of the intervention, some rodent and human studies have revealed that *Fgf-21* administration leads to improvement in obesity-related metabolic complications [55–57]. Thus, indicating the pathological relevance of these batokines during the progression of T2D.

Furthermore, across different weeks of growth, dysfunctional adipose tissue is accompanied by increased production of pro-inflammatory cytokines, a decline of anti-inflammatory activity, and infiltration of macrophages [7]. Consistently with increased *Tnf-α* expression in WAT and BAT, our data also showed an age-related decrease in *Metrnl* expression with more severity in BAT of *db/db* mice, which could negatively influence the expression of thermogenic and anti-inflammatory genes [58]. Likewise, the expression of *Gdt-15* and *Cxcl-14* were also impaired in these *db/db* mice, indicating the impaired anti-inflammatory activity in BAT owing to the fact that both *Gdt-15* and *Cxcl-14* are involved in the recruitment of M2-type macrophage [59,60]. In sharp contrast, *Cxcl-14* promotes WAT browning and ameliorates glucose/insulin homeostasis in high-fat-diet-induced obese mice via M2 macrophage recruitment, and the lack of *Cxcl-14* impairs BAT activity and alters glucose homeostasis [59].

5. Study limitations

This study has some limitations to be acknowledged. Owing to time constraints and availability issues of some reagents and materials, we were not able to further verify gene expression results using Western blot analysis. Moreover, serum analysis of BAT secretory factors was also not carried out, something that would be of interest in a future study.

6. Conclusion and future perspective

Consistent with impaired metabolic function, the hypertrophy of BAT is associated with alteration in the expression pattern of batokines in obese-type 2 diabetic *db/db* mice. This pathogenetic process is aggravated with age and represents impaired regulation of genes involved in thermogenesis, inflammation, and glucose homeostasis. Further highlighting the significance of adipose tissue-derived factors such as adipokines and batokines for T2D-disease monitoring and therapeutic development or relevant agents. Ultimately, this will assist in the diagnosis and prediction of obesity and its related metabolic diseases.

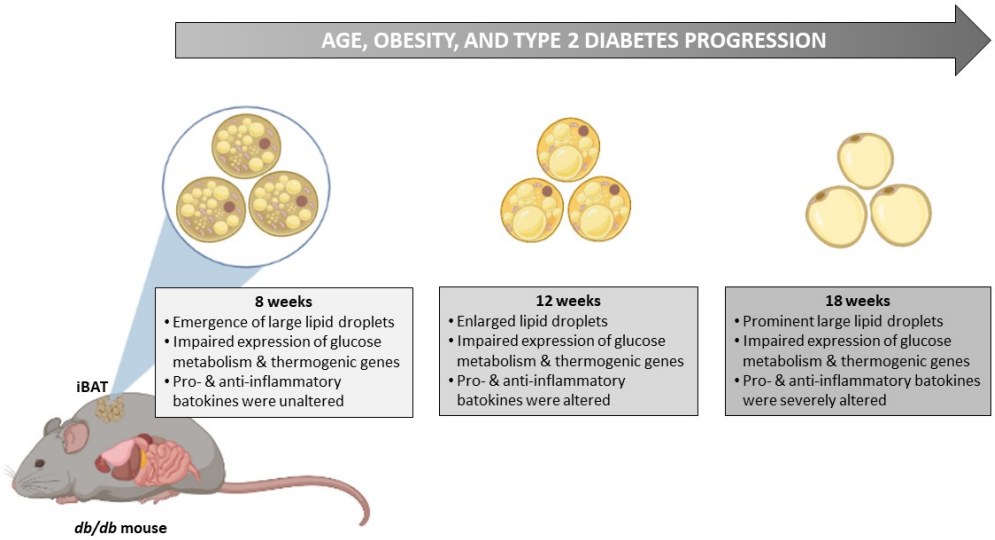

Figure 8: An overview of the alterations in the morphology and batokines gene expression pattern that reflects the progressive deterioration of the interscapular brown adipose tissue (iBAT) with the progression of age, obesity, and type 2 diabetes in *db/db* mice. In brief, iBAT displayed hypertrophy and acquired the white-like appearance (increased lipid droplet size) which was accompanied by impaired BAT-secreted factors "batokines" upon the progression of the disease in *db/db* mice with age.

Abbreviations

AdipoQ: Adiponectin, **BAT:** Brown adipose tissue, **BMP8b:** Bone morphogenetic protein 8b, **CXCL-14:** C-X-C motif chemokine ligand 14, **GLUT-4:** glucose transporter 4: **FGF-21**: Fibroblast growth factor 21, **GDF-15**: Growth differentiation factor 15, **METRNL:** Meteorin like, **NAFLD:** Non-alcoholic fatty liver disease, **NRG-4:** Neuregulin 4, **OGTT:** Oral glucose tolerance test, **T2D:** Type 2 diabetes, **TNF-α:** Tumour necrosis factor-alpha,

UCP-1: Uncoupling protein 1, **VEGFA:** Vascular endothelial growth factor A, **HOMA-IR:** Homeostasis model of assessment for insulin resistance, **WAT:** white adipose tissue

CRediT authorship contribution statement

K.Z, P.V.D, and S.E.M.-M—concept and original draft; K.Z, T.A.N., C.P. and M.T.M —investigations and data analysis; S.E.M.-M.—funding and resources; K.Z, P.V.D, M.T.M, T.A.N., C.P, B.U.J, B.N, and S.E.M.-M.—editing, reviewing and approval of the final draft. All authors have read and agreed to the published version of the manuscript.

Declaration of competing interest

The authors declare no conflict of interest.

Funding statement

This work was funded by the National Research Foundation (NRF) of South Africa Thuthuka Programme Grant 128296 and NRF support for rated scientist 113674 to S.E. Mazibuko-Mbeje. Baseline funding from the Biomedical Research and Innovation Platform of the South African Medical Research Council (SAMRC) and Northwest University is also acknowledged. Grant holders acknowledge that opinions, findings and conclusions, or recommendations expressed in any publication generated by the NRF or SAMRC-supported research are those of the authors and that the NRF or SAMRC accepts no liability whatsoever in this regard.

Acknowledgments

K. Ziqubu is funded by the SAMRC through its Division of Research Capacity Development under the internship scholarship programme from funding received from the South African National Treasury.

References

[1] IDF Diabetes Atlas 2021 | IDF Diabetes Atlas n.d. https://diabetesatlas.org/atlas/tenth-edition/ (accessed June 30, 2022).

[2] Song C, Gong W, Ding C, Wang R, Fang H, Liu A. Gene–Environment Interaction on Type 2 Diabetes Risk among Chinese Adults Born in Early 1960s. Genes 2022, Vol 13, Page 645 2022;13:645. https://doi.org/10.3390/GENES13040645.

[3] Zheng Y, Ley SH, Hu FB. Global aetiology and epidemiology of type 2 diabetes mellitus and its complications. Nature Reviews Endocrinology 2017 14:2 2017;14:88–98. https://doi.org/10.1038/nrendo.2017.151.

[4] Fryk E, Olausson J, Mossberg K, Strindberg L, Schmelz M, Brogren H, et al. Hyperinsulinemia and insulin resistance in the obese may develop as part of a homeostatic response to elevated free fatty acids: A mechanistic case-control and a population-based cohort study. EBioMedicine 2021;65:103264. https://doi.org/10.1016/J.EBIOM.2021.103264.

[5] Longo M, Zatterale F, Naderi J, Parrillo L, Formisano P, Raciti GA, et al. Adipose Tissue Dysfunction as Determinant of Obesity-Associated Metabolic Complications. Int J Mol Sci 2019;20. https://doi.org/10.3390/IJMS20092358.

[6] Sakers A, de Siqueira MK, Seale P, Villanueva CJ. Adipose-tissue plasticity in health and disease. Cell 2022;185:419–46. https://doi.org/10.1016/J.CELL.2021.12.016.

[7] Mancuso P, Bouchard B. The impact of aging on adipose function and adipokine synthesis. Front Endocrinol (Lausanne) 2019;10:137. https://doi.org/10.3389/FENDO.2019.00137/BIBTEX.

[8] Mahlangu T, Dludla P v., Nyambuya TM, Mxinwa V, Mazibuko-Mbeje SE, Cirilli I, et al. A systematic review on the functional role of Th1/Th2 cytokines in type 2 diabetes and related metabolic complications. Cytokine 2020;126. https://doi.org/10.1016/J.CYTO.2019.154892.

[9] Burhans MS, Hagman DK, Kuzma JN, Schmidt KA, Kratz M. Contribution of Adipose Tissue Inflammation to the Development of Type 2 Diabetes Mellitus. Compr Physiol 2019;9:1–58. https://doi.org/10.1002/CPHY.C170040.

[10] Guzmán-Ruiz R, Tercero-Alcázar C, Rabanal-Ruiz Y, Díaz-Ruiz A, el Bekay R, Rangel-Zuñiga OA, et al. Adipose tissue depot-specific intracellular and extracellular cues contributing to insulin resistance in obese individuals. FASEB J 2020;34:7520–39. https://doi.org/10.1096/FJ.201902703R.

[11] Nalliah CJ, Bell JR, Raaijmakers AJA, Waddell HM, Wells SP, Bernasochi GB, et al. Epicardial Adipose Tissue Accumulation Confers Atrial Conduction Abnormality. J Am Coll Cardiol 2020;76:1197–211. https://doi.org/10.1016/J.JACC.2020.07.017.

[12] Liu Y, Jin J, Chen Y, Chen C, Chen Z, Xu L. Integrative analyses of biomarkers and pathways for adipose tissue after bariatric surgery. Adipocyte 2020;9:384–400. https://doi.org/10.1080/21623945.2020.1795434.

[13] Suchacki KJ, Stimson RH. Nutritional Regulation of Human Brown Adipose Tissue. Nutrients 2021, Vol 13, Page 1748 2021;13:1748. https://doi.org/10.3390/NU13061748.

[14] Pilkington AC, Paz HA, Wankhade UD. Beige Adipose Tissue Identification and Marker Specificity-Overview. Front Endocrinol (Lausanne) 2021;12. https://doi.org/10.3389/FENDO.2021.599134.

[15] Singh R, Barrios A, Dirakvand G, Pervin S. Human Brown Adipose Tissue and Metabolic Health: Potential for Therapeutic Avenues. Cells 2021, Vol 10, Page 3030 2021;10:3030. https://doi.org/10.3390/CELLS10113030.

[16] Saito M. Brown Adipose Tissue as a Therapeutic Target for Obesity: From Mice to Humans. The Korean Journal of Obesity 2015;24:1–8. https://doi.org/10.7570/KJO.2015.24.1.1.

[17] Carey AL, Kingwell BA. Brown adipose tissue in humans: Therapeutic potential to combat obesity. Pharmacol Ther 2013;140:26–33. https://doi.org/10.1016/J.PHARMTHERA.2013.05.009.

[18] Vidal P, Stanford KI. Exercise-Induced Adaptations to Adipose Tissue Thermogenesis. Front Endocrinol (Lausanne) 2020;11. https://doi.org/10.3389/FENDO.2020.00270.

[19] Cedikova M, Kripnerová M, Dvorakova J, Pitule P, Grundmanova M, Babuska V, et al. Mitochondria in White, Brown, and Beige Adipocytes. Stem Cells Int 2016;2016. https://doi.org/10.1155/2016/6067349.

[20] Ahmad B, Vohra MS, Saleemi MA, Serpell CJ, Fong IL, Wong EH. Brown/Beige adipose tissues and the emerging role of their secretory factors in improving metabolic health: The batokines. Biochimie 2021;184:26–39. https://doi.org/10.1016/J.BIOCHI.2021.01.015.

[21] Kaisanlahti A, Glumoff T. Browning of white fat: agents and implications for beige adipose tissue to type 2 diabetes. J Physiol Biochem 2019;75:1–10. https://doi.org/10.1007/S13105-018-0658-5/TABLES/1.

[22] Mazibuko-Mbeje SE, Ziqubu K, Dludla P v., Tiano L, Silvestri S, Orlando P, et al. Isoorientin ameliorates lipid accumulation by regulating fat browning in palmitate-exposed 3T3-L1 adipocytes. Metabol Open 2020;6:100037. https://doi.org/10.1016/J.METOP.2020.100037.

[23] Roth CL, Molica F, Kwak BR, Alvarez-Llamas G, Martin-Lorenzo M. Browning of White Adipose Tissue as a Therapeutic Tool in the Fight against Atherosclerosis. Metabolites 2021, Vol 11, Page 319 2021;11:319. https://doi.org/10.3390/METABO11050319.

[24] Otero-Díaz B, Rodríguez-Flores M, Sánchez-Muñoz V, Monraz-Preciado F, Ordoñez-Ortega S, Becerril-Elias V, et al. Exercise Induces White Adipose Tissue Browning Across the Weight Spectrum in Humans. Front Physiol 2018;9:1781. https://doi.org/10.3389/FPHYS.2018.01781/BIBTEX.

[25] Salgado ALFDA, de Carvalho L, Oliveira AC, dos Santos VN, Vieira JG, Parise ER. Insulin resistance index (HOMA-IR) in the differentiation of patients with non-alcoholic fatty liver disease and healthy individuals. Arq Gastroenterol 2010;47:165–9. https://doi.org/10.1590/S0004-28032010000200009.

[26] Pan XX, Yao KL, Yang YF, Ge Q, Zhang R, Gao PJ, et al. Senescent T Cell Induces Brown Adipose Tissue "Whitening" Via Secreting IFN-γ. Front Cell Dev Biol 2021;9:277. https://doi.org/10.3389/FCELL.2021.637424/BIBTEX.

[27] Du K, Bai X, Yang L, Shi Y, Chen L, Wang H, et al. De Novo Reconstruction of Transcriptome Identified Long Non-Coding RNA Regulator of Aging-Related Brown Adipose Tissue Whitening in Rabbits. Biology 2021, Vol 10, Page 1176 2021;10:1176. https://doi.org/10.3390/BIOLOGY10111176.

[28] Rangel-Azevedo C, Santana-Oliveira DA, Miranda CS, Martins FF, Mandarim-de-Lacerda CA, Souza-Mello V. Progressive brown adipocyte dysfunction: Whitening and impaired nonshivering thermogenesis as long-term obesity complications. J Nutr Biochem 2022;105:109002. https://doi.org/10.1016/J.JNUTBIO.2022.109002.

[29] Wang GX, Zhao XY, Lin JD. The brown fat secretome: metabolic functions beyond thermogenesis. Trends in Endocrinology & Metabolism 2015;26:231–7. https://doi.org/10.1016/J.TEM.2015.03.002.

[30] Gonçalves LF, Machado TQ, Castro-Pinheiro C, de Souza NG, Oliveira KJ, Fernandes-Santos C. Ageing is associated with brown adipose tissue remodelling and loss of white fat browning in female C57BL/6 mice. Int J Exp Pathol 2017;98:100–8. https://doi.org/10.1111/IEP.12228.

[31] Lecoultre V, Ravussin E. Brown adipose tissue and aging. Curr Opin Clin Nutr Metab Care 2011;14:1–6. https://doi.org/10.1097/MCO.0B013E328341221E.

[32] Dalbøge LS, Almholt DLC, Neerup TSR, Vassiliadis E, Vrang N, Pedersen L, et al. Characterisation of Age-Dependent Beta Cell Dynamics in the Male db/db Mice. PLoS One 2013;8:e82813. https://doi.org/10.1371/JOURNAL.PONE.0082813.

[33] Burke SJ, Batdorf HM, Burk DH, Noland RC, Eder AE, Boulos MS, et al. Db / db Mice Exhibit Features of Human Type 2 Diabetes That Are Not Present in Weight-Matched C57BL/6J Mice Fed a Western Diet. J Diabetes Res 2017;2017. https://doi.org/10.1155/2017/8503754.

[34] Bruno MEC, Mukherjee S, Powell WL, Mori SF, Wallace FK, Balasuriya BK, et al. Accumulation of γδ T cells in visceral fat with aging promotes chronic inflammation. Geroscience 2022;44:1761–78. https://doi.org/10.1007/S11357-022-00572-W.

[35] Ghosh AK, O'Brien M, Mau T, Qi N, Yung R. Adipose Tissue Senescence and Inflammation in Aging is Reversed by the Young Milieu. J Gerontol A Biol Sci Med Sci 2019;74:1709–15. https://doi.org/10.1093/GERONA/GLY290.

[36] Alcalá M, Calderon-Dominguez M, Bustos E, Ramos P, Casals N, Serra D, et al. Increased inflammation, oxidative stress and mitochondrial respiration in brown adipose tissue from obese mice. Sci Rep 2017;7. https://doi.org/10.1038/S41598-017-16463-6.

[37] Jeong JH, Chang JS, Jo YH. Intracellular glycolysis in brown adipose tissue is essential for optogenetically induced nonshivering thermogenesis in mice. Sci Rep 2018;8. https://doi.org/10.1038/S41598-018-25265-3.

[38] Carpentier AC, Blondin DP, Virtanen KA, Richard D, Haman F, Turcotte ÉE. Brown Adipose Tissue Energy Metabolism in Humans. Front Endocrinol (Lausanne) 2018;9. https://doi.org/10.3389/FENDO.2018.00447.

[39] Burke SJ, Batdorf HM, Burk DH, Noland RC, Eder AE, Boulos MS, et al. db/ db Mice Exhibit Features of Human Type 2 Diabetes That Are Not Present in Weight-Matched C57BL/6J Mice Fed a Western Diet. J Diabetes Res 2017;2017. https://doi.org/10.1155/2017/8503754.

[40] el Khoury NB, Gratuze M, Petry F, Papon MA, Julien C, Marcouiller F, et al. Hypothermia mediates age-dependent increase of tau phosphorylation in db/db mice. Neurobiol Dis 2016;88:55–65. https://doi.org/10.1016/J.NBD.2016.01.005.

[41] Dalbøge LS, Almholt DLC, Neerup TSR, Vassiliadis E, Vrang N, Pedersen L, et al. Characterisation of age-dependent beta cell dynamics in the male db/db mice. PLoS One 2013;8. https://doi.org/10.1371/JOURNAL.PONE.0082813.

[42] Mestres-Arenas A, Villarroya J, Giralt M, Villarroya F, Peyrou M. A Differential Pattern of Batokine Expression in Perivascular Adipose Tissue Depots From Mice. Front Physiol 2021;12:714530. https://doi.org/10.3389/FPHYS.2021.714530/FULL.

[43] Oana F, Takeda H, Matsuzawa A, Akahane S, Isaji M, Akahane M. Adiponectin receptor 2 expression in liver and insulin resistance in db/db mice given a beta3-adrenoceptor agonist. Eur J Pharmacol 2005;518:71–6. https://doi.org/10.1016/J.EJPHAR.2005.06.004.

[44] Gibbs EM, Stock JL, McCoid SC, Stukenbrok HA, Pessin JE, Stevenson RW, et al. Glycemic improvement in diabetic db/db mice by overexpression of the human insulin-regulatable glucose transporter (GLUT4). J Clin Invest 1995;95:1512–8. https://doi.org/10.1172/JCI117823.

[45] Abel ED, Peroni O, Kim JK, Kim YB, Boss O, Hadro E, et al. Adipose-selective targeting of the GLUT4 gene impairs insulin action in muscle and liver. Nature 2001;409:729–33. https://doi.org/10.1038/35055575.

[46] Im SS, Kwon SK, Kang SY, Kim TH, Kim H il, Hur MW, et al. Regulation of GLUT4 gene expression by SREBP-1c in adipocytes. Biochemical Journal 2006;399:131. https://doi.org/10.1042/BJ20060696.

[47] Alcalá M, Calderon-Dominguez M, Bustos E, Ramos P, Casals N, Serra D, et al. Increased inflammation, oxidative stress and mitochondrial respiration in brown adipose tissue from obese mice. Scientific Reports 2017 7:1 2017;7:1–12. https://doi.org/10.1038/s41598-017-16463-6.

[48] Shimizu I, Aprahamian T, Kikuchi R, Shimizu A, Papanicolaou KN, MacLauchlan S, et al. Vascular rarefaction mediates whitening of brown fat in obesity. J Clin Invest 2014;124:2099. https://doi.org/10.1172/JCI71643.

[49] Kotzbeck P, Giordano A, Mondini E, Murano I, Severi I, Venema W, et al. Brown adipose tissue whitening leads to brown adipocyte death and adipose tissue inflammation. J Lipid Res 2018;59:784–94. https://doi.org/10.1194/JLR.M079665.

[50] Pellegrinelli V, Peirce VJ, Howard L, Virtue S, Türei D, Senzacqua M, et al. Adipocyte-secreted BMP8b mediates adrenergic-induced remodeling of the neuro-vascular network in adipose tissue. Nature Communications 2018 9:1 2018;9:1–18. https://doi.org/10.1038/s41467-018-07453-x.

[51] Whittle AJ, Carobbio S, Martins L, Slawik M, Hondares E, Vázquez MJ, et al. BMP8B Increases Brown Adipose Tissue Thermogenesis through Both Central and Peripheral Actions. Cell 2012;149:871–85. https://doi.org/10.1016/J.CELL.2012.02.066.

[52] Wang GX, Zhao XY, Meng ZX, Kern M, Dietrich A, Chen Z, et al. The brown fat-enriched secreted factor Nrg4 preserves metabolic homeostasis through attenuation of hepatic lipogenesis. Nat Med 2014;20:1436–43. https://doi.org/10.1038/NM.3713.

[53] Shimizu I, Aprahamian T, Kikuchi R, Shimizu A, Papanicolaou KN, MacLauchlan S, et al. Vascular rarefaction mediates whitening of brown fat in obesity. J Clin Invest 2014;124:2099–112. https://doi.org/10.1172/JCI71643.

[54] Serdan TDA, Masi LN, Pereira JNB, Rodrigues LE, Alecrim AL, Scervino MVM, et al. Impaired brown adipose tissue is differentially modulated in insulin-resistant obese wistar and type 2 diabetic Goto-Kakizaki rats. Biomedicine & Pharmacotherapy 2021;142:112019. https://doi.org/10.1016/J.BIOPHA.2021.112019.

[55] Li H, Wu G, Fang Q, Zhang M, Hui X, Sheng B, et al. Fibroblast growth factor 21 increases insulin sensitivity through specific expansion of subcutaneous fat. Nature Communications 2018 9:1 2018;9:1–16. https://doi.org/10.1038/s41467-017-02677-9.

[56] Geng L, Liao B, Jin L, Huang Z, Triggle CR, Ding H, et al. Exercise Alleviates Obesity-Induced Metabolic Dysfunction via Enhancing FGF21 Sensitivity in Adipose Tissues. Cell Rep 2019;26:2738-2752.e4. https://doi.org/10.1016/J.CELREP.2019.02.014.

[57] Bernardo B, Lu M, Bandyopadhyay G, Li P, Zhou Y, Huang J, et al. FGF21 does not require interscapular brown adipose tissue and improves liver metabolic profile in animal models of obesity and insulin-resistance. Scientific Reports 2015 5:1 2015;5:1–13. https://doi.org/10.1038/srep11382.

[58] Rao RR, Long JZ, White JP, Svensson KJ, Lou J, Lokurkar I, et al. Meteorin-like Is a Hormone that Regulates Immune-Adipose Interactions to Increase Beige Fat Thermogenesis. Cell 2014;157:1279–91. https://doi.org/10.1016/J.CELL.2014.03.065.

[59] Cereijo R, Gavaldà-Navarro A, Cairó M, Quesada-López T, Villarroya J, Morón-Ros S, et al. CXCL14, a Brown Adipokine that Mediates Brown-Fat-to-Macrophage Communication in Thermogenic Adaptation. Cell Metab 2018;28:750-763.e6. https://doi.org/10.1016/J.CMET.2018.07.015.

[60] Campderrós L, Moure R, Cairó M, Gavaldà-Navarro A, Quesada-López T, Cereijo R, et al. Brown Adipocytes Secrete GDF15 in Response to Thermogenic Activation. Obesity 2019;27:1606–16. https://doi.org/10.1002/OBY.22584.